



Thio- and aminocaffeine analogues as inhibitors of human monoamine oxidase

Hermanus P. Booysen^a, Christina Moraal^a, Gisella Terre'Blanche^a, Anél Petzer^b, Jacobus J. Bergh^a,
Jacobus P. Petzer^{a,*}

^a Pharmaceutical Chemistry, School of Pharmacy, North-West University, Private Bag X6001, Potchefstroom 2520, South Africa

^b Unit for Drug Research and Development, School of Pharmacy, North-West University, Private Bag X6001, Potchefstroom 2520, South Africa

ARTICLE INFO

Article history:

Received 26 August 2011

Revised 4 October 2011

Accepted 13 October 2011

Available online 20 October 2011

Keywords:

Monoamine oxidase

Reversible inhibition

Caffeine

Sulfanylcaffeine

Thiocaffeine

Aminocaffeine

ABSTRACT

In a recent study it was shown that 8-benzyloxycaffeine analogues act as potent reversible inhibitors of human monoamine oxidase (MAO) A and B. Although the benzyloxy side chain appears to be particularly favorable for enhancing the MAO inhibition potency of caffeine, a variety of other C8 oxy substituents of caffeine also lead to potent MAO inhibition. In an attempt to discover additional C8 substituents of caffeine that lead to potent MAO inhibition and to explore the importance of the ether oxygen for the MAO inhibition properties of C8 oxy-substituted caffeines, a series of 8-sulfanyl- and 8-aminocaffeine analogues were synthesized and their human MAO-A and -B inhibition potencies were compared to those of the 8-oxycaffeines. The results document that the sulfanylcaffeine analogues are reversible competitive MAO-B inhibitors with potencies comparable to those of the oxycaffeines. The most potent inhibitor, 8-[[[(4-bromophenyl)methyl]sulfanyl]caffeine, exhibited an IC_{50} value of 0.167 μ M towards MAO-B. While the sulfanylcaffeine analogues also exhibit affinities for MAO-A, they display in general a high degree of MAO-B selectivity. The aminocaffeine analogues, in contrast, proved to be weak MAO inhibitors with a number of analogues exhibiting no binding to the MAO-A and -B isozymes. The results of this study are discussed with reference to possible binding orientations of selected caffeine analogues within the active site cavities of MAO-A and -B. MAO-B selective sulfanylcaffeine derived inhibitors may act as lead compounds for the design of antiparkinsonian therapies.

© 2011 Elsevier Ltd. All rights reserved.

1. Introduction

The monoamine oxidases (MAO) A and B are mitochondrial bound flavin adenine dinucleotide (FAD) enzymes which catalyze the α -carbon oxidation of a variety of aminyl substrates.¹ Human MAO-A and -B consist of 529 and 520 amino acids, respectively, and the FAD is covalently bound to a cysteinyl residue in both enzymes (Cys-406 and Cys-397 in MAO-A and -B, respectively). While MAO-A and -B are products of separate genes they share approximately 70% amino acid sequence identity.² The X-ray crystallographic structures of MAO-A and -B indicate that the amino acid residues comprising the active sites and their relative geometries are similar with only 6 of the 16 active site amino acid residues differing between the two enzymes.^{3,4} In spite of these similarities, MAO-A and -B have different substrate and inhibitor specificities. Most notably, MAO-A metabolizes the neurotransmitters, serotonin and norepinephrine, as well as the dietary amine, tyramine. MAO-B is well known to metabolize extraneous amines such as benzylamine and phenylethylamine. Dopamine is considered to be a substrate for both isozymes.⁵

Since MAO-A and -B are both involved in the degradation of neurotransmitter amines, inhibitors of these enzymes are employed as

drugs in the treatment of several disorders.⁵ For example, MAO-A inhibitors block the central oxidation of serotonin by MAO-A and are used as antidepressants. MAO-B inhibitors reduce the MAO-B catalyzed oxidative metabolism of dopamine in the brain and are used in the treatment of Parkinson's disease. Of importance is the observation that MAO-B activity and density increase in most brain regions including the basal ganglia with age while MAO-A activity remains unchanged.^{6,7} In the aged parkinsonian brain MAO-B is therefore thought to be the principal MAO isozyme responsible for dopamine catabolism. MAO-B inhibitors may conserve dopamine in the basal ganglia and offer a symptomatic benefit in the treatment of Parkinson's disease.^{8–10} MAO-B inhibitors are frequently combined with levodopa therapy since inhibitors of this enzyme have been shown to enhance the elevation of dopamine levels derived from levodopa.¹¹ MAO-B inhibitors may permit a reduction of the dose of levodopa required for a therapeutic effect and therefore the occurrence of levodopa associated side effects.¹² MAO may also play an important role in the neurodegenerative processes associated with Parkinson's disease. The oxidation of dopamine by MAO stoichiometrically yields potentially toxic metabolic by-products.¹³ For each mole of dopamine oxidized by MAO, one mole of hydrogen peroxide (which may lead to oxidative damage) and dopaldehyde (which may react with exocyclic amino groups of nucleosides and N-terminal and lysine ϵ -amino groups of proteins) are formed.¹³ Inhibitors of MAO reduce the MAO-catalyzed

* Corresponding author. Tel.: +27 18 2992206; fax: +27 18 2994243.

E-mail address: jacques.petzer@nwu.ac.za (J.P. Petzer).

metabolism of DA and as a result reduce the formation of these toxic by-products. MAO inhibitors are therefore considered as a potential treatment strategy to slow the progression of Parkinson's disease since they may exert neuroprotective effects in the brain.¹³

Based on the therapeutic value of MAO inhibitors the current study aims to discover new reversible inhibitors of the MAO enzymes, particularly the B isozyme. For this purpose caffeine (**1**) serve as lead compound (Fig. 1). Although caffeine is a weak MAO-B inhibitor ($K_i = 3.6$ mM), substitution at the C8 position with a variety of substituents has been shown to enhance the MAO-B inhibition potency of caffeine to a large degree.¹⁴ In previous studies it was shown that substitution at C8 of caffeine with alkyloxy

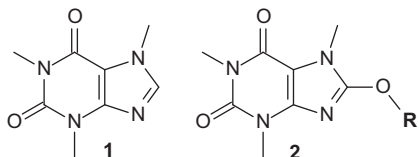


Figure 1. The structures of caffeine (**1**) and oxycaffeine analogues (**2**).

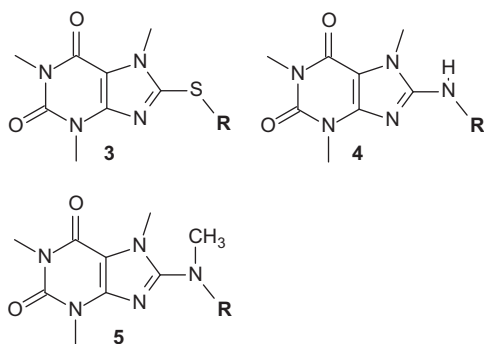


Figure 2. The structures of sulfanylcaffeine analogues (**3**), aminocaffeine analogues (**4**) and aminomethylcaffeine analogues (**5**).

Table 1

The IC_{50} values for the inhibition of recombinant human MAO-A and -B by compounds **3a–l**

	R	IC_{50}^a (μ M)		SI^b
		MAO-A	MAO-B	
3a	-S-C ₆ H ₅	56.4 ± 12.9	33.2 ± 3.41	1.7
3b	-S-CH ₂ -C ₆ H ₅	8.22 ± 1.13	1.86 ± 0.034	4.4
3c	-S-(CH ₂) ₂ -C ₆ H ₅	20.5 ± 4.49	0.223 ± 0.010	91.9
3d	-S-(CH ₂) ₂ -O-C ₆ H ₅	15.5 ± 2.17	0.332 ± 0.033	46.7
3e	-S-CH ₂ -(4-Cl-C ₆ H ₄)	2.77 ± 0.570	0.192 ± 0.025	14.4
3f	-S-CH ₂ -(4-Br-C ₆ H ₄)	2.62 ± 0.104	0.167 ± 0.020	15.7
3g	-S-CH ₂ -(4-F-C ₆ H ₄)	4.80 ± 0.584	0.348 ± 0.036	13.8
3h	-S-CH ₂ -(4-CH ₃ O-C ₆ H ₄)	— ^c	— ^c	—
3i	-S-(CH ₂) ₂ -CH(CH ₃) ₂	15.2 ± 4.09	2.62 ± 0.546	5.8
3j	-S-C ₆ H ₁₁	24.4 ± 8.76	13.1 ± 3.49	1.9
3k	-S-C ₅ H ₉	9.40 ± 0.572	20.9 ± 3.11	0.4
3l	-S-2-Naphthalenyl	3.60 ± 0.291	3.60 ± 1.10	1.0

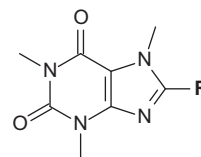
^a All values are expressed as the mean ± SD of triplicate determinations.

^b The selectivity index is the selectivity for the MAO-B isoform and is given as the ratio of IC_{50} (MAO-A)/ IC_{50} (MAO-B).

^c No inhibition observed at a maximum concentration of 100 μ M of the test inhibitor.

Table 2

The IC_{50} values for the inhibition of recombinant human MAO-A and -B by compounds **4a–h**



	R	IC_{50}^a (μ M)		SI^b
		MAO-A	MAO-B	
4a	-NH-C ₆ H ₅	— ^c	— ^c	—
4b	-NH-CH ₂ -C ₆ H ₅	— ^c	— ^c	—
4c	-NH-(CH ₂) ₂ -C ₆ H ₅	45.2 ± 9.19	17.6 ± 2.48	2.6
4d	-NH-(CH ₂) ₃ -C ₆ H ₅	— ^c	— ^c	—
4e	-NH-(CH ₂) ₄ -C ₆ H ₅	30.9 ± 6.74	9.60 ± 0.759	3.2
4f	-NH-(CH ₂) ₂ -(pyridin-2-yl)	— ^c	19.4 ± 5.07	—
4g	-NH-(CH ₂) ₂ -(3-ClC ₆ H ₄)	5.78 ± 0.411	24.4 ± 18.0	0.2
4h	-NH-C ₅ H ₉	— ^c	— ^c	—

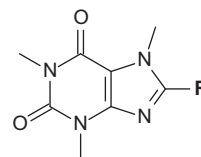
^a All values are expressed as the mean ± SD of triplicate determinations.

^b The selectivity index is the selectivity for the MAO-B isoform and is given as the ratio of IC_{50} (MAO-A)/ IC_{50} (MAO-B).

^c No inhibition observed at a maximum concentration of 100 μ M of the test inhibitor.

Table 3

The IC_{50} values for the inhibition of recombinant human MAO-A and -B by compounds **5a–b**



	R	IC_{50}^a (μ M)		SI^b
		MAO-A	MAO-B	
5a	-(NCH ₃)-(CH ₂) ₂ -C ₆ H ₅	107 ± 9.85	16.8 ± 6.83	6.4
5b	-(NCH ₃)-(CH ₂) ₄ -C ₆ H ₅	37.7 ± 6.40	2.97 ± 0.536	12.7

^a All values are expressed as the mean ± SD of triplicate determinations.

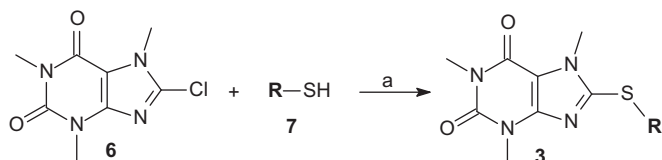
^b The selectivity index is the selectivity for the MAO-B isoform and is given as the ratio of IC_{50} (MAO-A)/ IC_{50} (MAO-B).

substituents (**2**) yielded particularly potent MAO-B inhibitors with a number of compounds exhibiting IC_{50} values in the nM range.^{15,16} Interestingly these oxycaffeines are also MAO-A inhibitors, a property that may be attributed to the relatively large degree of rotational freedom of the C8 side chain at the carbon-oxygen ether bond. It has been suggested that structures with a relatively larger degree of conformational freedom may be better suited for binding to MAO-A than relatively rigid structures.¹⁵ Based on these promising results the present study investigates the possibility that alkylsulfanyl and alkylamino substituents at C8 of caffeine may similarly enhance the MAO-A and -B inhibition potency of caffeine. For this purpose, a series of 12 aryl- and alkylsulfanylcaffeine analogues (**3a–l**) and 10 aryl- and alkylaminocaffeine analogues (**4a–h**, **5a–b**) were synthesized and evaluated as potential inhibitors of recombinant human MAO-A and -B (Fig. 2 and Tables 1–3).

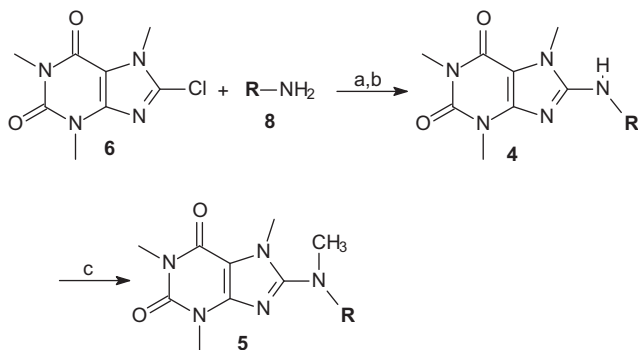
2. Results

2.1. Chemistry

The aryl- and alkylsulfanylcaffeine analogues (**3a–l**) were synthesized by reacting 8-chlorocaffeine (**6**) with an appropriate



Scheme 1. Synthetic pathway to sulfanylcaffeine analogues (**3**). Reagents and conditions: (a) NaOH, H₂O/ethanol, reflux.



Scheme 2. Synthetic pathway to aminocaffeine analogues (**4** and **5**). Reagents and conditions: (a) reflux; (b) acetic acid; (c) KOH, DMSO, CH₃I.

thiol reagent (**7**) in the presence of NaOH and employing a mixture of ethanol and water as reaction solvent (Scheme 1).¹⁷ The aryl- and alkylaminocaffeine analogues (**4a–h**) were similarly prepared by reaction of an appropriate amine reagent (**8**) with 8-chlorocaffeine but with the exception that the addition of base and additional solvent were not required (Scheme 2).¹⁸ Methylation of **4c** and **4e** at the C8 amine to yield aminomethyl caffeine analogues **5a** and **5b**, respectively, were carried out in DMSO using CH₃I as alkylating agent and KOH as base. The structures of all the target compounds were verified by ¹H NMR, ¹³C NMR and mass spectrometry. The purities of the compounds were estimated by HPLC analysis.

2.2. Inhibition of MAO-A and -B

The MAO inhibition potencies of the sulfanylcaffeine (**3a–l**) and aminocaffeine analogues (**4a–h**, **5a–b**) were examined by employing the recombinant human MAO-A and -B enzymes as enzyme sources.¹⁹ The mixed MAO-A/B substrate, kynuramine, was used as substrate for the inhibition studies of both MAO-A and -B. Kynuramine displays similar *K_m* values towards the two enzymes with values of 16.1 and 22.7 μM for MAO-A and -B, respectively.¹⁵ The MAO-catalyzed oxidation of kynuramine yields 4-hydroxyquinoline, a fluorescent compound which is readily measured in basic solutions at excitation and emission wavelengths of 310 and 400 nm, respectively. Neither the substrate nor the test inhibitors fluoresce under these conditions, or quench the fluorescence of 4-hydroxyquinoline. The inhibition potencies of the sulfanylcaffeine and aminocaffeine analogues are expressed as the IC₅₀ values which were determined from sigmoidal dose–response curves constructed in triplicate from six different inhibitor concentrations spanning at least 3 orders of magnitude.

2.2.1. MAO inhibition by sulfanylcaffeine analogues (**3a–l**)

The MAO inhibition potencies of the sulfanylcaffeine analogues (**3a–l**) are presented in Table 1. As shown by the selectivity index (SI) values, the sulfanylcaffeine analogues are selective inhibitors of MAO-B. The only exceptions are **3k** which displays slight selectivity for the MAO-A isozyme and **3l** which is essentially

nonselective. 8-(Phenylsulfanyl)caffeine (**3a**) which displays slight selectivity for MAO-B, was found to be a relatively weak inhibitor of both MAO-A and -B. Extension of the C8 side chain by one methylene unit to yield the benzylsulfanyl homolog **3b** (IC₅₀ = 1.86 μM) enhances the MAO-B inhibition potency 17-fold compared to **3a** (IC₅₀ = 33.2 μM). A further increase in the length of the C8 side chain yields even more potent MAO-B inhibitors. For example, compounds **3c** and **3d**, the phenylethylsulfanyl and phenoxyethylsulfanyl homologs exhibited IC₅₀ values of 0.223 and 0.332 μM, respectively. While the extension of the C8 side chain of **3a** (IC₅₀ = 56.4 μM) by one methylene unit to yield **3b** (IC₅₀ = 8.22 μM) also results in improved MAO-A inhibition, further increasing the length of the C8 side chain does not result in a further enhancement of inhibition activity. For example, **3c** (IC₅₀ = 20.5 μM) and **3d** (IC₅₀ = 15.5 μM) are weaker MAO-A inhibitors than the benzylsulfanyl homolog **3b** (IC₅₀ = 8.22 μM).

Interestingly, halogen substitution of the phenyl ring of the C8 side chain is also associated with an increase in MAO-B inhibition potency. The benzylsulfanyl substituted caffeine homologs containing chlorine (**3e**; IC₅₀ = 0.192 μM), bromine (**3f**; IC₅₀ = 0.167 μM) and fluorine (**3g**; IC₅₀ = 0.348 μM) on the benzyl phenyl ring were found to be 5- to 11-fold more potent than the corresponding unsubstituted homolog **3b** (IC₅₀ = 1.86 μM). Methoxy substitution of the phenyl ring of 8-(benzylsulfanyl)caffeine, in contrast, is associated with a loss of both MAO-A and -B inhibition activity. Halogen substitution of 8-(benzylsulfanyl)caffeine (**3b**) also enhances MAO-A inhibition potency, although by a lesser degree compared to MAO-B. The homologs containing chlorine (**3e**; IC₅₀ = 2.77 μM), bromine (**3f**; IC₅₀ = 2.62 μM) and fluorine (**3g**; IC₅₀ = 4.80 μM) on the benzyl phenyl ring are 1.7- to 3-fold more potent than the corresponding unsubstituted homolog **3b** (IC₅₀ = 8.22 μM).

The results document that compound **3i**, the sulfanylcaffeine analogue containing a branched alkyl side chain at C8, is also a relatively good MAO-B inhibitor with an IC₅₀ value of 2.62 μM. In fact, **3i** is approximately 12-fold more potent as an MAO-B inhibitor than was 8-(phenylsulfanyl)caffeine (**3a**) which contains a C8 phenylsulfanyl side chain. This result demonstrates that a ring system in the C8 side chain is not an absolute requirement for MAO-B inhibition by sulfanylcaffeine analogues. In accordance with this view, compound **3i** also proved to be more potent as a MAO-B inhibitor than the sulfanylcaffeine analogues containing cyclohexyl (**3j**), cyclopentyl (**3k**) and naphthalenyl (**3l**) C8 side chains. Interestingly the sulfanylcaffeine analogues containing cyclohexyl (**3j**), cyclopentyl (**3k**) and naphthalenyl (**3l**) C8 side chains were more potent inhibitors of both MAO-A and -B than the phenyl substituted analogue **3a**. This result suggests that, with the appropriate structural modification, these moieties may be suitable for the future design of sulfanylcaffeine derived MAO inhibitors. An example of such a structural modification would be the extension of the length of the C8 side chain. Based on the observations that the naphthalenyl substituted sulfanylcaffeine analogue **3l** is 15- and 9-fold more potent as a MAO-A and -B inhibitor, respectively, than the phenyl substituted sulfanylcaffeine analogue **3a** and that **3l** is a nonselective inhibitor, the naphthalenyl moiety may be particularly suited for the design of sulfanylcaffeine derived mixed MAO-A/B inhibitors.

2.2.2. MAO inhibition by aminocaffeine analogues (**4a–h**, **5a–b**)

The MAO inhibition potencies of the aminocaffeine analogues **4a–h** are presented in Tables 2 and 3. The data show that these compounds were relatively weak inhibitors of both MAO-A and -B with IC₅₀ values ranging from 5.78–45.2 to 9.60–24.4 μM for the inhibition of MAO-A and -B, respectively. In fact, several of the compounds exhibited no binding and the MAO-A and -B isozymes. Even homologs containing extended C8 side chains such as **4d** (–NH–(CH₂)₃–C₆H₅) and **4e** (–NH–(CH₂)₄–C₆H₅) did not

exhibit potent MAO inhibition. Similarly, homolog **4g**, which contains a halogen on the phenyl ring of the C8 side chain, was found to be a relatively weak MAO inhibitor. These results demonstrate that, in contrast to the sulfanylcaffeine analogues, extension of the length of the C8 side chain and halogen substitution do not lead to potent MAO-B inhibition by the aminocaffeine analogues. Compared to the sulfanylcaffeine analogues, the aminocaffeine analogues are therefore weak MAO-B inhibitors. For example, sulfanylcaffeine analogue **3c** ($IC_{50} = 0.223 \mu\text{M}$) is 78-fold more potent as an MAO-B inhibitor than its corresponding aminocaffeine homolog **4c** ($IC_{50} = 17.6 \mu\text{M}$).

To investigate the possibility of enhancing the MAO inhibition potencies of the aminocaffeines, selected analogues, **4c** and **4e**, were methylated at the C8 amine to yield compounds **5a** and **5b**, respectively. While methylation improved the MAO-B inhibition potency of **4e** by approximately 3-fold, MAO-A inhibition activity was slightly reduced. Methylation of **4c** did not result in a significant improvement of MAO-B inhibition potency and led to a reduction in MAO-A inhibition. Compared to the sulfanylcaffeine analogues, the aminocaffeine analogues are also weak MAO-B inhibitors. For example, sulfanylcaffeine analogue **3c** ($IC_{50} = 0.223 \mu\text{M}$) is 75-fold more potent than its aminomethylcaffeine homolog **5a** ($IC_{50} = 16.8 \mu\text{M}$). It is noteworthy that the most potent MAO-B inhibitor among the aminocaffeine analogues was the C8 methylated derivative **5b** with an IC_{50} value of $2.97 \mu\text{M}$. It can therefore be concluded that while methylation of the C8 amine of aminocaffeine analogues may result in enhanced MAO-B inhibition potency, the resulting compounds remain relatively weak inhibitors compared to the sulfanylcaffeine analogues.

2.3. Reversibility of MAO-A and -B inhibition

Based on the nature of the interactions with the MAO enzymes, inhibitors may be classified as reversible or irreversible. Irreversible inhibitors normally form covalent interactions with the enzymes while reversible inhibitors bind via intermolecular interactions. While irreversible inhibitors of MAO have been clinically used for many years, this mode of inhibition may be associated with certain shortcomings.²⁰ These include a slow and variable recovery of enzyme activity following withdrawal of the irreversible inhibitor.²¹ The turnover rate for the biosynthesis of MAO-B in the human brain may be as much as 40 days.²² In contrast, enzyme activity is regained relatively quickly following withdrawal of a reversible inhibitor, once the inhibitor is cleared from the tissues. Based on these observations, the reversibility of MAO-A and -B inhibition by the sulfanylcaffeine and aminocaffeine analogues was examined. For this purpose the time-dependency of the inhibition of MAO-A and -B, respectively, by sulfanylcaffeine analogue **3f** was measured. The time-dependency of the inhibition of MAO-A and -B by aminocaffeine analogues **4g** and **5b**, respectively, was also examined. While irreversible inhibitors would lead to a time-dependent reduction of enzyme activity, the degree of enzyme inhibition in the presence of a reversible MAO inhibitor remains unchanged irrespective of the time for which the inhibitor is incubated with the enzyme.²³

The test inhibitors, at concentrations of approximately 2-fold their measured IC_{50} values for the inhibition of the respective MAO enzymes, were preincubated with recombinant human MAO-A or -B for time periods of 0, 15, 30 and 60 min. Following these preincubations the residual MAO catalytic activities were measured after the addition of the substrate, kynuramine. The results of these reversibility studies are presented in Figures 3 and 4. The graphs show that when **3f** and **4g** are preincubated with MAO-A and **3f** and **5b** are preincubated with MAO-B there are no time-dependent reductions of MAO-A and -B catalytic activities. Even after a period of 60 min the test compounds do not reduce

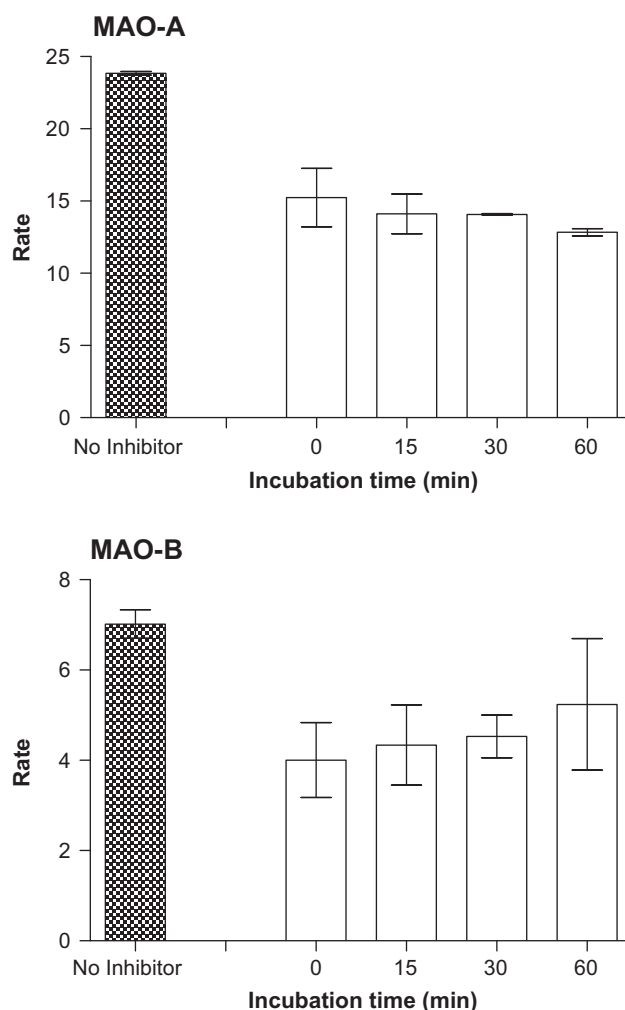


Figure 3. Time-dependent inhibition of recombinant human MAO-A and -B by **3f**. The enzymes were preincubated for various periods of time (0–60 min) with **3f** at concentrations of 5.22 and 0.32 μM for MAO-A and -B, respectively. The concentrations of the enzyme substrate, kynuramine, were 45 and 30 μM for the studies with MAO-A and MAO-B, respectively, and the enzyme concentrations were 0.015 mg/mL. The catalytic rates are expressed as nmoles 4-hydroxyquinoline formed/min/mg protein.

the MAO catalytic rates. These results suggest that the test caffeines are not time-dependent inhibitors of MAO-A and -B and interact reversibly, at least for the time period (0–60 min) and at the inhibitor concentrations ($2 \times IC_{50}$) evaluated.

This study also examined the possibility that **3f** may act as a competitive inhibitor of human MAO-A and -B. For this purpose, sets of Lineweaver–Burk plots were constructed for the inhibition of these enzymes by **3f**. The initial catalytic rates of MAO-A or -B were measured in the absence and presence of three different concentrations of **3f**. These measurements were carried out using four different concentrations of the substrate, kynuramine (15–90 μM). The Lineweaver–Burk plots obtained from these experiments are shown in Figure 5. The graphs show that the Lineweaver–Burk plots constructed for the inhibition of MAO-A and -B are linear and intersect at the y-axis. This indicates that the inhibition of the MAO enzymes by **3f** is competitive. This result is further support that **3f** is a reversible MAO inhibitor.

2.4. Molecular modeling

The results of the MAO inhibition studies shows that among the sulfanylcaffeine analogues evaluated here, several compounds act

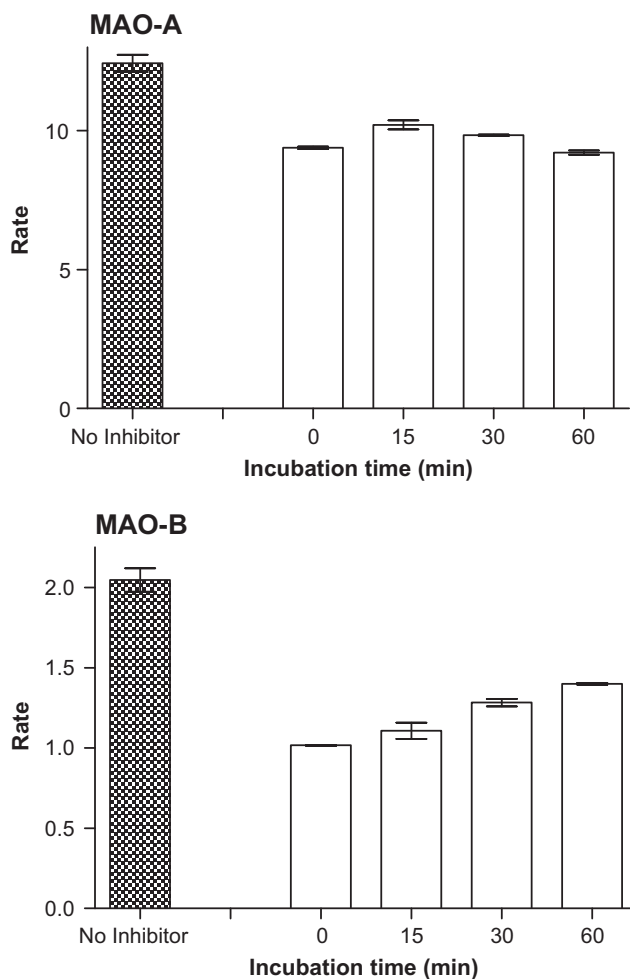


Figure 4. Time-dependent inhibition of recombinant human MAO-A and -B by **4g** and **5b**, respectively. The enzymes were preincubated for various periods of time (0–60 min) with **4g** (MAO-A) and **5b** (MAO-B) at concentrations of 11.56 and 5.94 μM , respectively. The concentrations of the enzyme substrate, kynuramine, were 45 and 30 μM for the studies with MAO-A and MAO-B, respectively, and the enzyme concentrations were 0.0075 mg/mL. The catalytic rates are expressed as nmoles 4-hydroxyquinoline formed/min/mg protein.

as potent reversible inhibitors of MAO-B with IC_{50} values in the nM range. Interestingly, extension of the length of the C8 side chain leads to enhanced MAO-B inhibition potency. While the sulfanylcaffeine analogues are also MAO-A inhibitors, they display, for the most part, selectivity for the MAO-B isozyme. In contrast to the sulfanylcaffeine analogues, the aminocaffeine analogues were found to be weak MAO-B inhibitors with many analogues exhibiting no binding to either MAO-A or -B. To provide additional insight, the predicted binding modes of selected analogues (**3a–c** and **4c**) in the active site cavities of MAO-A and -B were examined using molecular docking.

The docking studies were carried out using the LigandFit application of the Discovery Studio modeling software (Accelrys) according to a previously reported protocol.²³ As enzyme models, the three-dimensional structures of human MAO-A cocrystallized with harmine (PDB entry: 2Z5X)³ and human MAO-B cocrystallized with safinamide (PDB entry: 2V5Z)⁴ were selected. The enzyme models were prepared by calculating the protonation states of the ionizable residues and adding the hydrogen atoms accordingly. After the valences of the FAD cofactor and cocrystallized ligands were corrected, hydrogen atoms were added and the models were subjected to an energy minimization cascade while

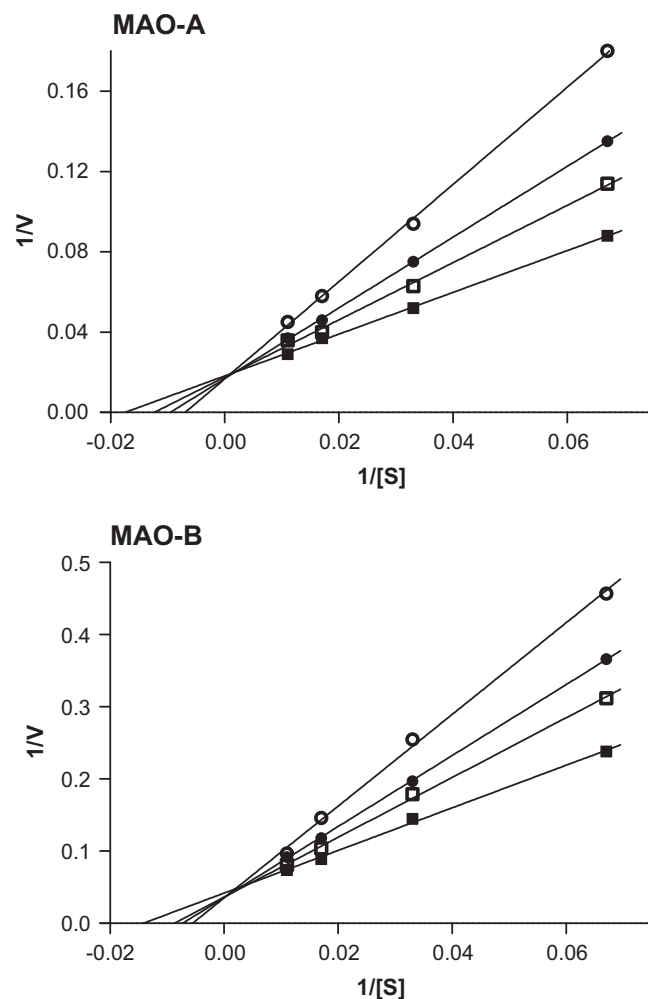


Figure 5. Lineweaver-Burk plots of the recombinant human MAO-A and -B catalyzed oxidation of kynuramine in the absence (filled squares) and presence of various concentrations of **3f**. For the studies with MAO-A the concentrations of **3f** were: 1.31 μM (open squares), 2.61 μM (filled circles), 5.22 μM (open circles). For the studies with MAO-B the concentrations of **3f** were: 0.04 μM (open squares), 0.08 μM (filled circles), 0.16 μM (open circles). The rates (V) are expressed as nmol product formed/min/mg protein.

the protein backbone was constrained. For the purpose of the docking, only the crystal waters, which are reported to be conserved and non-displaceable, were retained (see Section 4).^{3,4}

The best ranked docking solution for the binding of the selected analogues (**3a–c** and **4c**) to MAO-B shows one prevailing orientation for all of the inhibitors. As shown by the binding orientation of **3c**, the caffeine ring binds within the substrate cavity of MAO-B, in close proximity to the FAD cofactor (Fig. 6). This places the carbonyl oxygen at C2 of the caffeine ring 3.4 Å from the flavin N5 and the carbonyl oxygen at C6 within hydrogen bond distance to the phenolic hydrogen of Tyr-435. The caffeine ring also forms a potential π - π interaction with the aromatic ring of Tyr-398. The region defined by the flavin isoalloxazine ring, Tyr-398 and Tyr-435 is the only polar space of the MAO-B active site and is also the site where amine catalysis occurs.²⁴ In the MAO-B model selected for these studies, the side chain of Ile-199 is rotated into an alternative conformation to allow for the fusion of the substrate and entrance cavities.²⁵ This rotation of the Ile-199 side chain from the active site cavity is essential for relatively large inhibitors, such as safinamide and C8 substituted caffeine derivatives, to be able to bind to MAO-B. As a result the phenylethyl C8 side chain of **3c** is

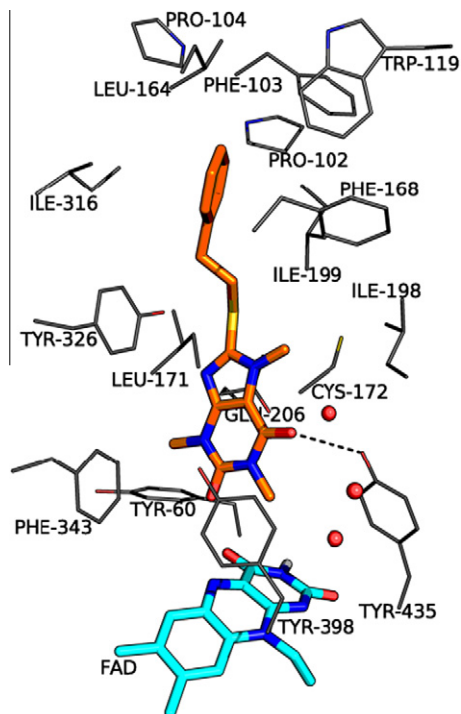


Figure 6. The predicted binding orientation of **3c** (orange) in the MAO-B active site.

allowed to extend into the hydrophobic entrance cavity where it may be stabilized via Van der Waals interactions. As expected, the relatively shorter phenyl (**3a**) and benzyl (**3b**) C8 side chains of sulfanylcaffeine homologs **3a** and **3b** do not extend as deep into the MAO-B entrance cavity as the side chain of **3c**, and may therefore undergo interactions with the entrance cavity to a lesser extent compared to **3c** (Fig. 7). Despite the similar binding

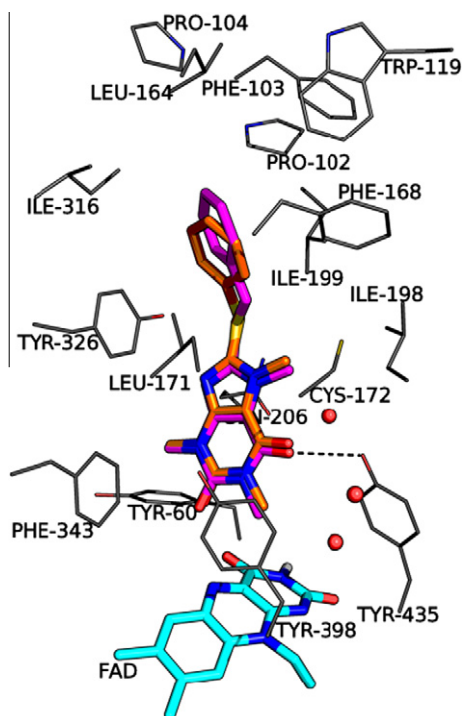


Figure 7. The predicted binding orientations of **3a** (orange) and **3b** (magenta) in the MAO-B active site.

orientations of **3a** and **3b** within the MAO-B active site, **3b** was found to be a 17-fold more potent inhibitor. Since **3b** protrudes only slightly deeper (by ~ 1.2 Å) into the entrance cavity compared to **3a**, this result suggests that a relatively small enhancement of the space occupied by an inhibitor in the entrance cavity leads to a large increase in binding affinity. Another possible explanation may be that the larger degree of conformational freedom afforded by the longer C8 side chain of **3b** may facilitate improved interaction with the entrance cavity. The view that interaction with the entrance cavity is essential for high affinity inhibitor binding is supported by the observation that caffeine is a weak MAO-B inhibitor.¹⁴ Lacking a C8 side chain, caffeine is expected to bind only within the substrate cavity and is unable to interact with the entrance cavity. The lower MAO-B inhibition potencies of **3a** and **3b** compared to compound **3c** may thus be explained by weaker interaction with the entrance cavity.

Interestingly the aminocaffeine analogue **4c** adopts a similar binding mode to that described above for **3c** and as a result forms similar interactions with the MAO-B active site (Fig. 8). The only additional interaction that may occur between **4c** and MAO-B is a potential hydrogen bond between the C8 amine and the phenolic group of Tyr-326. The results of the MAO inhibition studies however, document that the aminocaffeine analogues are weak MAO-B inhibitors with **4c** being 78-fold weaker than the corresponding sulfanylcaffeine homolog **3c**. The docking studies therefore suggest that differing binding orientations cannot account for the apparent loss of MAO-B inhibition activity of the aminocaffeine analogues.

The predicted binding orientation of **3c** within the active site of MAO-A is similar to the binding orientation observed in MAO-B, with the caffeine ring bound in close proximity to the FAD cofactor and the C8 side chain extending towards the entrance of the active site (Fig. 9). Interestingly, the caffeine ring is rotated by $\sim 180^\circ$ compared to the binding orientation adopted in the MAO-B active site. This dissimilarity in binding orientations in the MAO-A and -B active sites has also been observed in docking studies with 8-benzylxocaffeine ana-

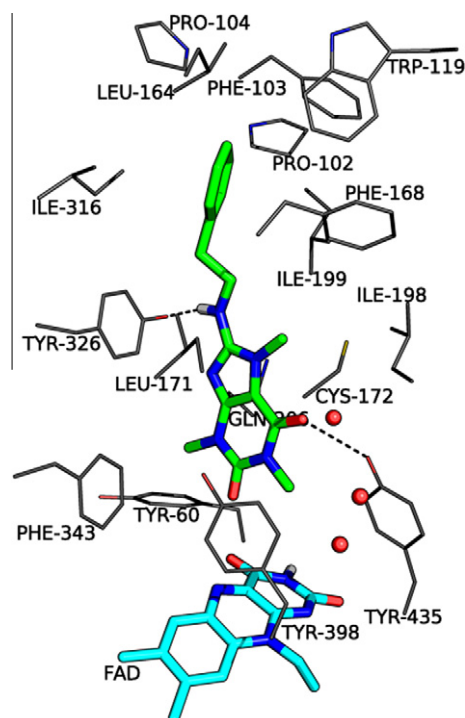


Figure 8. The predicted binding orientation of **4c** (green) in the MAO-B active site.

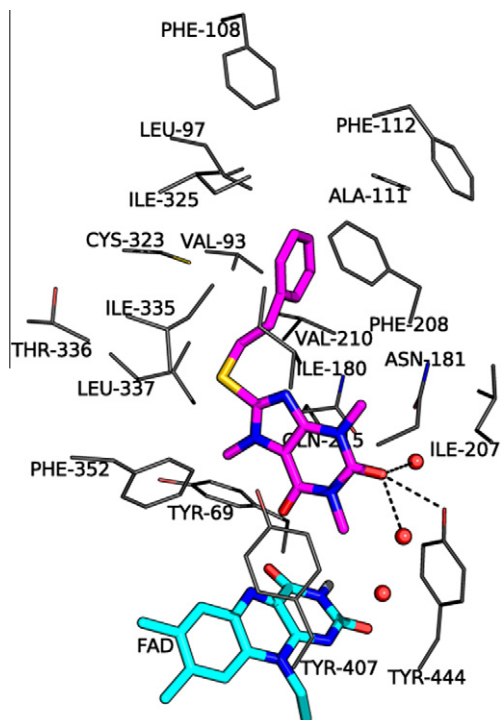


Figure 9. The predicted binding orientation of **3c** (magenta) in the MAO-A active site.

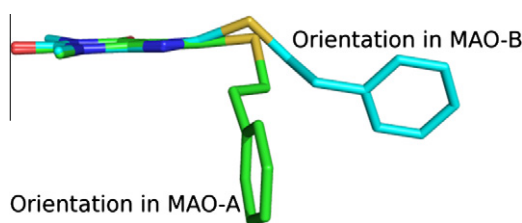


Figure 10. The predicted binding orientations of **3c** within the active sites of MAO-A (green) and MAO-B (cyan) with the caffeine moieties of the respective orientations overlaid.

logues.¹⁵ As a result of the flipped orientation of the caffeine ring, the C2 carbonyl oxygen is within hydrogen bond distance of the phenolic hydrogen of Tyr-444 and two active site waters. Also, the caffeine ring of **3c** binds more distant from Tyr-407 (~4.3 Å) in MAO-A than from the corresponding residue, Tyr-398 (~3.6 Å), in MAO-B. For this reason, a π - π interaction similar to that observed between the caffeine ring and Tyr-398 in MAO-B, is not observed between **3c** and the MAO-A active site. This may represent a possible reason for the finding that sulfanylcaffeine analogues are in general more potent MAO-B inhibitors than MAO-A inhibitors. Also noteworthy is the observation that, in the MAO-A active site, the C8 side chain of **3c** is bent at the CH₂-S thioether bond from the plane of the caffeine ring while in the MAO-B active site, the side chain of **3c** exhibits a modest deviation from the plane of the caffeine ring (Fig. 10). The differing binding orientations adopted by C8 substituted caffeine derivatives in MAO-A and -B may, for the most part, be attributed to steric hindrance caused by the aromatic moieties of Phe-208 in MAO-A and Tyr-326 in MAO-B. As illustrated in Figure 11A, the binding orientation and position of **3c** in the MAO-B active site cannot be reproduced in MAO-A because this would result in structural overlap with the phenyl ring of Phe-208. In MAO-B,

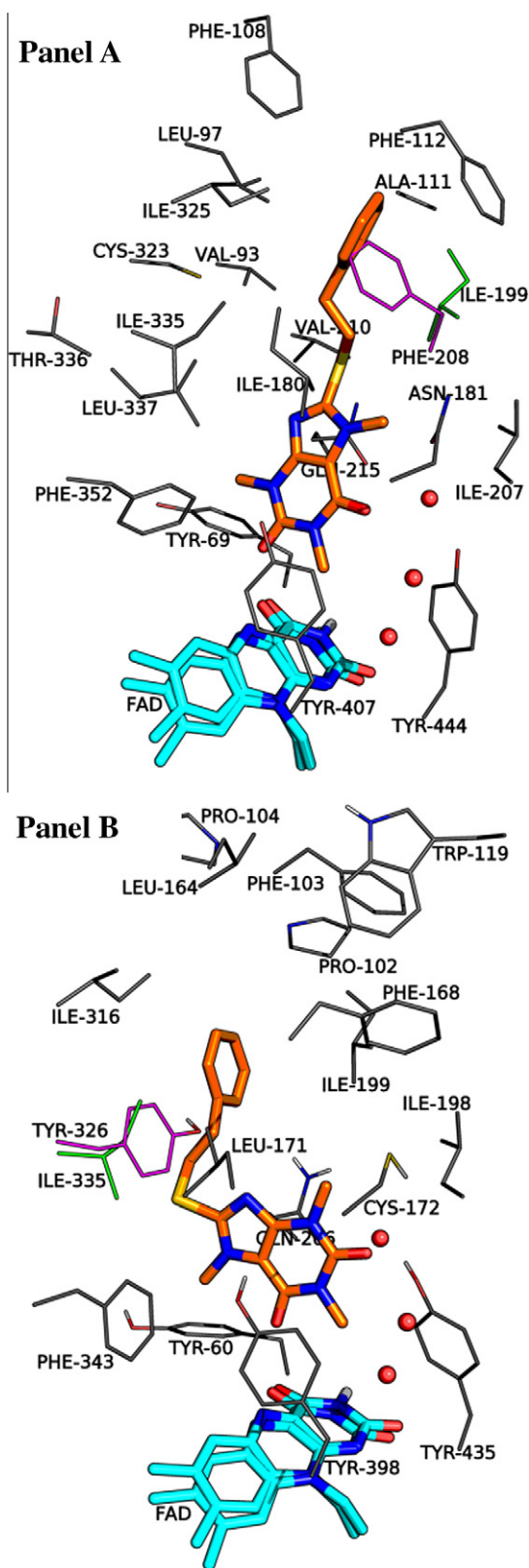


Figure 11. Illustrations of the overlaid active sites of human MAO-A and -B. Panel A: The predicted binding orientation of **3c** as docked within the active site of MAO-B is shown in the MAO-A active site. The active site residues of MAO-A are displayed in gray with Phe-208 in magenta while residue Ile-199 in MAO-B is displayed in green. Panel B: The predicted binding orientation of **3c** as docked within the active site of MAO-A is shown in the MAO-B active site. The active site residues of MAO-B are displayed in gray with Tyr-326 in magenta while residue Ile-325 in MAO-A is displayed in green.

the amino acid residue that occupies the same position as Phe-208 in MAO-A is Ile-199. In MAO-B the side chain of Ile-199 may rotate out of the active site cavity to allow for the observed binding pose of **3c**.²⁵ Similarly, the binding orientation and position of **3c** in the MAO-A active site cannot be reproduced in MAO-B because of structural overlap with of Tyr-326 (Fig. 11B). In MAO-A, the amino acid residue that occupies the analogous position as Tyr-398 in MAO-B is Ile-335. The relatively smaller side chain of Ile-335 compared to the aromatic ring of Tyr-398, does not sterically prevent the observed binding orientation of **3c** in the MAO-A active site.³

3. Discussion

Based on previous reports that oxycaffeine analogues are MAO inhibitors,^{15,16} the present study investigated the possibility that C8 substituted sulfanylcaffeine and aminocaffeine analogues may also act as inhibitors of human MAO-A and -B. The results demonstrated that several of the sulfanylcaffeine analogues act as potent MAO-B inhibitors and that the inhibition is reversible. For example, the bromine substituted sulfanylcaffeine analogue **3f** was the most potent MAO-B inhibitor with an IC₅₀ value of 0.167 μM. The relatively high MAO-B inhibition potencies of the sulfanylcaffeine analogues may be evaluated by comparison of the IC₅₀ value of **3f** (IC₅₀ = 0.167 μM) with the reversible inhibitor safinamide, which binds to MAO-B with an IC₅₀ value of 0.08 μM.⁴ While the sulfanylcaffeine analogues are also MAO-A inhibitors, they are for the most part selective for the MAO-B isoform. Modeling studies predict that the sulfanylcaffeine analogues adopt dissimilar binding modes in the MAO-A and -B active site cavities, respectively. Compared to the predicted orientation in MAO-B, the caffeine ring is flipped by approximately 180° in the MAO-A active site which results in differing interactions of the caffeine ring with the polar regions of the MAO-A and -B substrate cavities. The alternative binding orientation of the caffeine ring in MAO-A may be less optimal for the formation of stabilizing polar interactions compared to the binding orientation adopted in MAO-B and may explain, at least in part, the lower binding affinities of the sulfanylcaffeine analogues to MAO-A.¹⁵ Interestingly, modeling studies suggest that the C8 side chain of the sulfanylcaffeine analogue **3c** is bent to a high degree from the plane of the caffeine ring at the CH₂-S thioether bond while in the MAO-B active site, the C8 side chain displays only a modest deviation from the plane of the caffeine moiety. The ability of the C8 side chain to adopt a bent orientation may be an important requirement for the inhibition of MAO-A. Rigid C8 substituted caffeine analogues such as (*E*)-8-(3-chlorostyryl)caffeine (CSC) (Fig. 12) are not MAO-A inhibitors while displaying high affinity binding to MAO-B.²⁶ The observation that CSC does not bind to MAO-A may be explained by its low degree of flexibility and inability to adopt a bent orientation similar to that observed for **3c** in the MAO-A active site.

The notion that the C8 side chains of the caffeine analogues are important structural features for MAO-A and -B inhibition is supported by the observation that caffeine is a weak MAO inhibitor.¹⁴ Modeling shows that, in the MAO-B active site, the C8 side chains of the sulfanylcaffeine analogues may extend into the hydrophobic

entrance cavity where they are stabilized by Van der Waals interactions. Since extension of the C8 chain length results in enhanced MAO-B inhibition potency, it may be concluded that longer C8 side chains form more productive interactions with the MAO-B entrance cavity, which thus leads to more potent enzyme inhibition. Halogen substitution on the phenyl ring of the C8 side chain also leads to a significant enhancement of MAO-B inhibition. This result may be explained by the possibility that halogen substitution may further improve Van der Waals and dipole interactions between the MAO-B entrance cavity and the C8 side chain. While it is not clear why methoxy substitution of 8-(benzylsulfanyl)caffeine leads to a loss of both MAO-A and -B inhibition potency, this result is in accordance with the findings of a previous study, which showed that MAO-B inhibition potencies of a series of benzylloxycaine analogues correlate with the electronegativity of substituents on the phenyl ring of the C8 side chain and that electron-withdrawing groups enhance MAO-B inhibition potency.¹⁵ Interestingly, this study shows that C8 side chains that do not contain phenyl rings are also suitable for MAO inhibition. Examples of sulfanylcaffeine analogues containing such side chains are the 3-methylbutyl (**3i**), cyclohexyl (**3j**), cyclopentyl (**3k**) and naphthalenyl (**3l**) substituted homologs.

One of the most significant findings of this study is that the aminocaffeine analogues are weak MAO inhibitors with most homologs displaying no inhibition. The predicted binding orientation and interactions of aminocaffeine analogue **4c** in the MAO-B active site is similar to the orientation of sulfanylcaffeine analogue **3c**. In fact **4c** displays an additional hydrogen bond interaction with Tyr-326. In spite of these predictions, **4c** is approximately 78-fold weaker as a MAO-B inhibitor compared to **3c**. Even methylation of the C8 amines to yield tertiary amines does not produce inhibitors with similar potencies to those of the sulfanylcaffeine analogues. While the reasons for this behavior is not clear, differing ionization states of the sulfanylcaffeine and aminocaffeine analogues do not explain the difference in binding affinities to the MAO enzymes, since both the sulfanylcaffeine and aminocaffeine analogues are expected to be uncharged in the buffer used for the inhibition studies (pH 7.4). Also, it is unlikely that aminocaffeines are excluded from entering the access channel leading to the active site cavity since aminyl substrates are thought to be deprotonated prior to entering the MAO active sites.²⁴

In conclusion, the sulfanylcaffeine analogues exhibit similar MAO-B inhibition potencies to those of the previously reported oxycaine analogues with various homologs from both series exhibiting IC₅₀ values in the nM range.^{15,16} The attachment of substituents at C8 of caffeine via a thioether linkage therefore enhances MAO-B inhibition activity to a similar extent compared to attachment via an oxyether. In contrast, C8 substituted aminocaffeines are not suitable for MAO inhibition. Based on the potent MAO-B inhibition properties of the sulfanylcaffeine analogues, they may be considered as lead compounds for the development of reversible MAO-B inhibitors.

4. Experimental section

4.1. Chemicals and instrumentation

Unless otherwise noted, all starting materials were obtained from Sigma-Aldrich and were used without purification. Proton (¹H) and carbon (¹³C) NMR spectra were recorded on a Bruker Avance III 600 spectrometer at frequencies of 600 and 150 MHz, respectively. All NMR measurements were conducted in CDCl₃ and DMSO-*d*₆ and the chemical shifts are reported in parts per million (δ) downfield from the signal of tetramethylsilane added to the deuterated solvent. Spin multiplicities are given as s (singlet), d (doublet), dd (doublet of doublets), t (triplet), q (quartet), qn

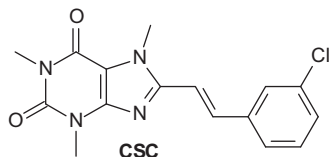


Figure 12. The structure of (*E*)-8-(3-chlorostyryl)caffeine (CSC).

(quintet), sept (septet) or m (multiplet). High resolution mass spectra (HRMS) were obtained on a Waters Synapt G2 instrument in electrospray ionization (ESI) mode. The HRMS spectrum of **4a** was recorded on a DFS high resolution magnetic sector mass spectrometer (Thermo Electron Corporation) in atmospheric pressure chemical ionization (APCI) mode. Melting points (mp) were measured with a Stuart SMP10 melting point apparatus and are uncorrected. The purity of the synthesized compounds were determined via HPLC analyses which were conducted with an Agilent 1100 HPLC system equipped with a quaternary gradient pump and an Agilent 1100 series diode array detector (see [Supplementary data](#)). HPLC grade acetonitrile (Merck) and Milli-Q water (Millipore) were used for the chromatography. For fluorescence spectrophotometry, a Varian Cary Eclipse fluorescence spectrophotometer was employed. Microsomes from insect cells containing recombinant human MAO-A and -B (5 mg/mL) and kynuramine-2HBr were obtained from Sigma-Aldrich.

4.2. Synthesis of C8-substituted thiocaffeine analogues (3a–I)

A solution of NaOH (4 mmol) in 3.5 mL water and 7 mL ethanol was cooled in an ice bath and the appropriate thiol (4 mmol) was added. The reaction mixture was stirred and 8-chlorocaffeine (4 mmol) was added in a single portion to yield a suspension. The reaction was heated under reflux for 60 min and then cooled on ice. The white precipitate was collected by filtration and washed with 30 mL ethanol. The product was recrystallized from 30 mL ethanol at room temperature and the crystals were washed with 30 mL ethanol.¹⁷

4.2.1. 8-(Phenylsulfanyl)caffeine (3a)

The title compound was prepared from thiophenol in a yield of 65.1%: mp 149 °C (ethanol). ¹H NMR (Bruker Avance III 600, CDCl₃) δ 3.37 (s, 3H), 3.54 (s, 3H), 3.90 (s, 3H), 7.32 (m, 5H); ¹³C NMR (Bruker Avance III 600, CDCl₃) δ 28.0, 29.9, 33.1, 109.5, 128.2, 129.6, 130.5, 130.9, 146.4, 148.0, 151.4, 154.9; ESI-HRMS *m/z*: calcd for C₁₄H₁₅N₄O₂S (MH⁺), 303.0916, found 303.0912; Purity (HPLC): 98%.

4.2.2. 8-(Benzylsulfanyl)caffeine (3b)

The title compound was prepared from benzyl mercaptan in a yield of 59%: mp 149 °C (ethanol). ¹H NMR (Bruker Avance III 600, CDCl₃) δ 3.35 (s, 3H), 3.57 (s, 3H), 3.69 (s, 3H), 4.42 (s, 2H), 7.27 (m, 3H), 7.31 (m, 2H); ¹³C NMR (Bruker Avance III 600, CDCl₃) δ 27.8, 29.7, 32.2, 37.4, 108.7, 127.9, 128.7, 128.9, 136.6, 148.3, 150.0, 151.5, 154.6; ESI-HRMS *m/z*: calcd for C₁₅H₁₇O₂N₄S (MH⁺), found 317.1073; Purity (HPLC): 99%.

4.2.3. 8-[(2-Phenylethyl)sulfanyl]caffeine (3c)

The title compound was prepared from phenylethyl mercaptan in a yield of 22.9%: mp 95 °C (ethanol). ¹H NMR (Bruker Avance III 600, CDCl₃) δ 3.04 (t, 2H, *J* = 7.9 Hz), 3.36 (s, 3H), 3.49 (t, 2H, *J* = 7.9 Hz), 3.55 (s, 3H), 3.78 (s, 3H), 7.21 (m, 3H), 7.29 (m, 2H); ¹³C NMR (Bruker Avance III 600, CDCl₃) δ 27.8, 29.7, 32.1, 33.8, 36.0, 108.5, 126.7, 128.5, 139.3, 148.5, 150.9, 151.5, 154.5; ESI-HRMS *m/z*: calcd for C₁₆H₁₉N₄O₂S, 331.1229 (MH⁺), found 331.1229; Purity (HPLC): 99%.

4.2.4. 8-[(2-Phenoxyethyl)sulfanyl]caffeine (3d)

The title compound was prepared from 2-phenoxyethanethiol in a yield of 43.9%: mp 114 °C (ethanol). ¹H NMR (Bruker Avance III 600, CDCl₃) δ 3.37 (s, 3H), 3.53 (s, 3H), 3.63 (t, 2H, *J* = 6.4 Hz), 3.83 (s, 3H), 4.30 (t, 2H, *J* = 6.4 Hz), 6.91 (d, 2H, *J* = 8.3 Hz), 6.94 (t, 1H, *J* = 7.2 Hz), 7.25 (m, 2H); ¹³C NMR (Bruker Avance III 600, CDCl₃) δ 27.8, 29.7, 31.5, 32.2, 66.3, 108.7, 114.5, 121.3, 129.5, 148.4, 150.3, 151.5, 154.5, 158.1; ESI-HRMS *m/z*: calcd for

C₁₆H₁₉N₄O₃S (MH⁺), 347.1176, found 347.1173; Purity (HPLC): 95%.

4.2.5. 8-[[4-(4-Chlorophenyl)methyl]sulfanyl]caffeine (3e)

The title compound was prepared from 4-chlorobenzyl mercaptan in a yield of 85.6%: mp 169 °C (ethanol). ¹H NMR (Bruker Avance III 600, CDCl₃) δ 3.36 (s, 3H), 3.56 (s, 3H), 3.73 (s, 3H), 4.40 (s, 2H), 7.26 (m, 4H); ¹³C NMR (Bruker Avance III 600, CDCl₃) δ 27.9, 29.7, 32.2, 36.4, 108.8, 128.8, 130.3, 133.8, 135.2, 148.3, 149.7, 151.5, 154.6; ESI-HRMS *m/z*: calcd for C₁₅H₁₆ClN₄O₂S (MH⁺), 351.0682, found 351.0679; Purity (HPLC): 97%.

4.2.6. 8-[[4-(4-Bromophenyl)methyl]sulfanyl]caffeine (3f)

The title compound was prepared from 4-bromobenzyl mercaptan in a yield of 82.0%: mp 166 °C (ethanol). ¹H NMR (Bruker Avance III 600, CDCl₃) δ 3.35 (s, 3H), 3.55 (s, 3H), 3.72 (s, 3H), 4.38 (s, 2H), 7.21 (d, 2H, *J* = 8.3 Hz), 7.40 (d, 2H, *J* = 8.3 Hz); ¹³C NMR (Bruker Avance III 600, CDCl₃) δ 27.8, 29.7, 32.2, 36.4, 108.7, 121.8, 130.6, 131.8, 135.8, 148.3, 149.6, 151.4, 154.5; ESI-HRMS *m/z*: calcd for C₁₅H₁₆BrN₄O₂S (MH⁺), 395.0177, found 395.0178; Purity (HPLC): 98%.

4.2.7. 8-[[4-(4-Fluorophenyl)methyl]sulfanyl]caffeine (3g)

The title compound was prepared from 4-fluorobenzyl mercaptan in a yield of 71.6%: mp 175 °C (ethanol). ¹H NMR (Bruker Avance III 600, CDCl₃) δ 3.35 (s, 3H), 3.55 (s, 3H), 3.72 (s, 3H), 4.40 (s, 2H), 6.96 (t, 2H, *J* = 8.3 Hz), 7.30 (q, 2H, *J* = 5.3 Hz); ¹³C NMR (Bruker Avance III 600, CDCl₃) δ 27.8, 29.7, 32.1, 36.4, 108.7, 115.6 (d), 130.6 (d), 132.4 (d), 148.3, 149.8, 151.4, 154.5, 161.4, 163.1; ESI-HRMS *m/z*: calcd for C₁₅H₁₆FN₄O₂S (MH⁺), 335.0976, found 335.0972; Purity (HPLC): 95%.

4.2.8. 8-[[4-(4-Methoxyphenyl)methyl]sulfanyl]caffeine (3h)

The title compound was prepared from 4-methoxybenzyl mercaptan in a yield of 90.5%: mp 159 °C (ethanol). ¹H NMR (Bruker Avance III 600, CDCl₃) δ 3.36 (s, 3H), 3.58 (s, 3H), 3.71 (s, 3H), 3.76 (s, 3H), 4.39 (s, 2H), 6.80 (d, 2H, *J* = 8.7 Hz), 7.24 (d, 2H, *J* = 8.7 Hz); ¹³C NMR (Bruker Avance III 600, CDCl₃) δ 27.8, 29.7, 32.1, 37.0, 55.3, 108.6, 114.1, 128.4, 130.2, 148.4, 150.2, 151.5, 154.6, 159.2; ESI-HRMS *m/z*: calcd for C₁₆H₁₉N₄O₃S (MH⁺), 347.1176, found 347.1171; Purity (HPLC): 94%.

4.2.9. 8-[(3-Methylbutyl)sulfanyl]caffeine (3i)

The title compound was prepared from 3-methyl-1-butanethiol in a yield of 35.3%: mp 79 °C (ethanol). ¹H NMR (Bruker Avance III 600, CDCl₃) δ 0.91 (d, 6H, *J* = 6.8 Hz), 1.59 (q, 2H, *J* = 7.9 Hz), 1.69 (sept, 1H, *J* = 6.8 Hz), 3.23 (t, 2H, *J* = 7.5 Hz), 3.34 (s, 3H), 3.51 (s, 3H), 3.79 (s, 3H); ¹³C NMR (Bruker Avance III 600, CDCl₃) δ 22.1, 27.4, 27.8, 29.6, 30.8, 32.1, 38.5, 108.4, 148.4, 151.3, 151.5, 154.5; ESI-HRMS *m/z*: calcd for C₁₃H₂₁N₄O₂S (MH⁺), 297.1385, found 297.1382; Purity (HPLC): 97%.

4.2.10. 8-(Cyclohexylsulfanyl)caffeine (3j)

The title compound was prepared from cyclohexanethiol in a yield of 37.2%: mp 133 °C (ethanol). ¹H NMR (Bruker Avance III 600, CDCl₃) δ 1.28 (m, 1H), 1.38 (m, 2H), 1.48 (m, 2H), 1.58 (m, 1H), 1.74 (m, 2H), 2.03 (m, 2H), 3.34 (s, 3H), 3.52 (s, 3H), 3.71 (m, 1H), 3.82 (s, 3H); ¹³C NMR (Bruker Avance III 600, CDCl₃) δ 25.4, 25.8, 27.8, 29.7, 32.3, 33.4, 47.2, 108.4, 148.4, 150.3, 151.5, 154.6; ESI-HRMS *m/z*: calcd for C₁₄H₂₁N₄O₂S (MH⁺), 309.1385, found 309.1385; Purity (HPLC): 99%.

4.2.11. 8-(Cyclopentylsulfanyl)caffeine (3k)

The title compound was prepared from cyclopentanethiol in a yield of 60.9%: mp 135 °C (ethanol). ¹H NMR (Bruker Avance III 600, CDCl₃) δ 1.63 (m, 4H), 1.76 (m, 2H), 2.15 (m, 2H), 3.34 (s,

3H), 3.51 (s, 3H), 3.80 (s, 3H), 3.99 (qn, 1H); ^{13}C NMR (Bruker Avance III 600, CDCl_3) δ 24.6, 27.8, 29.7, 32.2, 33.8, 46.4, 108.2, 148.5, 151.3, 151.5, 154.6; ESI-HRMS m/z : calcd for $\text{C}_{13}\text{H}_{19}\text{N}_4\text{O}_2\text{S}$ (MH^+), 295.1229, found 295.1233; Purity (HPLC): 95%.

4.2.12. 8-(Naphthalen-2-ylsulfanyl)caffeine (3I)

The title compound was prepared from 2-naphthalenethiol in a yield of 87.7%: mp 175 °C (ethanol). ^1H NMR (Bruker Avance III 600, CDCl_3) δ 3.37 (s, 3H), 3.53 (s, 3H), 3.91 (s, 3H), 7.35 (dd, 1H, $J = 1.9, 8.3$ Hz), 7.48 (m, 2H), 7.73 (m, 1H), 7.78 (m, 2H), 7.84 (s, 1H); ^{13}C NMR (Bruker Avance III 600, CDCl_3) δ 27.9, 29.8, 33.1, 109.5, 126.9, 127.0, 127.4, 127.5, 127.8, 127.9, 129.4, 129.7, 132.6, 133.6, 146.4, 148.0, 151.4, 154.9; ESI-HRMS m/z : calcd for $\text{C}_{18}\text{H}_{17}\text{N}_4\text{O}_2\text{S}$ (MH^+), 353.1072, found 353.1074; Purity (HPLC): 94%.

4.3. Synthesis of C8-substituted aminocaffeine analogues (4a–h)

A mixture of 8-chlorocaffeine (2 mmol) and the appropriate amine (10 mmol) was heated under reflux (175–180 °C) for 3 h. The reaction was cooled to room temperature and treated with 50 mL acetic acid (5%). The resulting suspension was stirred for 15 min at room temperature and the precipitate was collected by filtration. The product was dried at 60 °C and recrystallized twice from ethanol (30 mL) at 0 °C.¹⁸

4.3.1. 8-(Phenylamino)caffeine (4a)

The title compound was prepared from aniline and 8-chlorocaffeine in a yield of 24.2%: mp 164–265 °C (ethanol). ^1H NMR (Bruker Avance III 600, $\text{DMSO}-d_6$) δ 3.15 (s, 3H), 3.35 (s, 3H), 3.74 (s, 3H), 6.96 (t, 1H, $J = 7.5$ Hz), 7.29 (t, 2H, $J = 7.5$ Hz), 7.67 (d, 2H, $J = 8.3$ Hz), 9.07 (s, 1H); ^{13}C NMR (Bruker Avance III 600, $\text{DMSO}-d_6$) δ 27.3, 29.4, 30.5, 102.0, 118.1, 121.7, 128.7, 140.0, 147.2, 149.3, 150.9, 153.3; APCI-HRMS m/z : calcd for $\text{C}_{14}\text{H}_{15}\text{N}_5\text{O}_2$ (M^+), 285.1226, found 285.1230; Purity (HPLC): 98%.

4.3.2. 8-(Benzylamino)caffeine (4b)

The title compound was prepared from benzylamine and 8-chlorocaffeine in a yield of 74.0%: mp 230 °C (ethanol). ^1H NMR (Bruker Avance III 600, $\text{DMSO}-d_6$) δ 3.14 (s, 3H), 3.35 (s, 3H), 3.58 (s, 3H), 4.53 (d, 2H, $J = 5.6$ Hz), 7.23 (t, 1H, $J = 7.5$ Hz), 7.32 (t, 2H, $J = 7.5$ Hz), 7.36 (d, 2H, $J = 7.5$ Hz), 7.56 (t, 1H, $J = 5.6$ Hz); ^{13}C NMR (Bruker Avance III 600, $\text{DMSO}-d_6$) δ 27.1, 29.2, 29.8, 45.7, 102.0, 126.9, 127.4, 128.3, 139.6, 148.2, 150.9, 152.9, 154.0; ESI-HRMS m/z : calcd for $\text{C}_{15}\text{H}_{18}\text{N}_5\text{O}_2$ (MH^+), 300.1460, found 300.1459; Purity (HPLC): 99%.

4.3.3. 8-[(2-Phenylethyl)amino]caffeine (4c)

The title compound was prepared from 2-phenylethylamine and 8-chlorocaffeine in a yield of 68.3%: mp 221 °C (ethanol). ^1H NMR (Bruker Avance III 600, $\text{DMSO}-d_6$) δ 2.88 (t, 2H, $J = 7.2$ Hz), 3.14 (s, 3H), 3.32 (s, 3H), 3.49 (m, 2H), 3.51 (s, 3H), 7.11 (t, 1H, $J = 5.3$ Hz), 7.19 (t, 1H, $J = 7.2$ Hz), 7.22 (d, 2H, $J = 7.5$ Hz), 7.29 (t, 2H, $J = 7.5$ Hz); ^{13}C NMR (Bruker Avance III 600, $\text{DMSO}-d_6$) δ 27.1, 29.2, 29.7, 35.3, 44.1, 101.8, 126.1, 128.3, 128.7, 139.4, 148.3, 150.9, 152.9, 153.9; ESI-HRMS m/z : calcd for $\text{C}_{16}\text{H}_{20}\text{N}_5\text{O}_2$ (MH^+), 314.1617, found 314.1621; Purity (HPLC): 99%.

4.3.4. 8-[(3-Phenylpropyl)amino]caffeine (4d)

The title compound was prepared from 3-phenylpropylamine and 8-chlorocaffeine in a yield of 76.8%: mp 204–205 °C (ethanol). ^1H NMR (Bruker Avance III 600, $\text{DMSO}-d_6$) δ 1.88 (qn, 2H, 7.5 Hz), 2.64 (t, 2H, $J = 7.5$ Hz), 3.13 (s, 3H), 3.30 (s, 3H), 3.32 (m, 2H), 3.52 (s, 3H), 6.98 (t, 1H, $J = 5.3$ Hz), 7.16 (t, 1H, $J = 7.2$ Hz), 7.22 (d, 2H, $J = 7.5$ Hz), 7.26 (t, 2H, $J = 7.5$ Hz); ^{13}C NMR (Bruker Avance

III 600, $\text{DMSO}-d_6$) δ 27.1, 29.2, 29.7, 30.8, 32.3, 42.0, 101.8, 125.7, 128.2, 128.3, 141.7, 148.3, 150.9, 152.8, 154.1; ESI-HRMS m/z : calcd for $\text{C}_{17}\text{H}_{22}\text{N}_5\text{O}_2$ (MH^+), 328.1773, found 328.1774; Purity (HPLC): 99%.

4.3.5. 8-[(4-Phenylbutyl)amino]caffeine (4e)

The title compound was prepared from 4-phenylbutylamine and 8-chlorocaffeine in a yield of 63.0%: mp 179–180 °C (ethanol). ^1H NMR (Bruker Avance III 600, $\text{DMSO}-d_6$) δ 1.59 (m, 4H), 2.60 (t, 2H, $J = 7.2$ Hz), 3.13 (s, 3H), 3.30 (s, 3H), 3.32 (m, 2H), 3.51 (s, 3H), 6.94 (t, 1H, $J = 5.6$ Hz), 7.14 (t, 1H, $J = 7.2$ Hz), 7.18 (d, 2H, $J = 7.2$ Hz), 7.25 (t, 2H, $J = 7.2$ Hz); ^{13}C NMR (Bruker Avance III 600, $\text{DMSO}-d_6$) δ 27.1, 28.2, 28.8, 29.2, 29.7, 34.8, 42.2, 101.7, 125.6, 128.2, 128.3, 142.1, 148.3, 150.9, 152.8, 154.1; ESI-HRMS m/z : calcd for $\text{C}_{18}\text{H}_{24}\text{N}_5\text{O}_2$ (MH^+), 342.1930, found 342.1929; Purity (HPLC): 99%.

4.3.6. 8-[[2-(Pyridin-2-yl)ethyl]amino]caffeine (4f)

The title compound was prepared from 2-(2-pyridyl)ethylamine and 8-chlorocaffeine in a yield of 20.4%: mp 196–197 °C (ethanol). ^1H NMR (Bruker Avance III 600, $\text{DMSO}-d_6$) δ 3.03 (t, 2H, $J = 7.2$ Hz), 3.13 (s, 3H), 3.31 (s, 3H), 3.50 (s, 3H), 3.65 (q, 2H, 6.7 Hz), 7.10 (t, 1H, $J = 5.6$ Hz), 7.20 (t, 1H, $J = 5.6$ Hz), 7.26 (d, 1H, $J = 7.5$ Hz), 7.69 (t, 1H, $J = 7.5$ Hz), 8.49 (d, 1H, $J = 4.1$ Hz); ^{13}C NMR (Bruker Avance III 600, $\text{DMSO}-d_6$) δ 27.1, 29.2, 29.7, 37.5, 42.4, 101.8, 121.5, 123.2, 136.4, 148.3, 149.0, 150.9, 152.8, 153.9, 159.1; ESI-HRMS m/z : calcd for $\text{C}_{15}\text{H}_{19}\text{N}_6\text{O}_2$ (MH^+), 315.1569, found 315.1570; Purity (HPLC): 98%.

4.3.7. 8-[[2-(3-Chlorophenyl)ethyl]amino]caffeine (4g)

The title compound was prepared from 2-(3-chlorophenyl)ethanamine and 8-chlorocaffeine in a yield of 48.5%: mp 111–113 °C (ethanol). ^1H NMR (Bruker Avance III 600, $\text{DMSO}-d_6$) δ 2.88 (t, 2H, $J = 7.2$ Hz), 3.13 (s, 3H), 3.32 (s, 3H), 3.50 (s, 3H), 3.52 (m, 2H), 7.10 (t, 1H, $J = 5.6$ Hz), 7.18 (d, 1H, $J = 7.5$ Hz), 7.24 (d, 1H, $J = 8.3$ Hz), 7.29 (d, 1H, $J = 7.5$ Hz), 7.31 (s, 1H); ^{13}C NMR (Bruker Avance III 600, $\text{DMSO}-d_6$) δ 27.1, 29.2, 29.7, 34.8, 43.7, 101.8, 126.1, 127.5, 128.6, 130.1, 132.9, 142.0, 148.3, 150.9, 152.8, 153.8; ESI-HRMS m/z : calcd for $\text{C}_{16}\text{H}_{19}\text{N}_5\text{O}_2\text{Cl}$ (MH^+), 348.1227, found 348.1225; Purity (HPLC): 98%.

4.3.8. 8-(Cyclopentylamino)caffeine (4h)

The title compound was prepared from cyclopentylamine and 8-chlorocaffeine in a yield of 38.6%: mp 217–218 °C (ethanol). ^1H NMR (Bruker Avance III 600, $\text{DMSO}-d_6$) δ 1.52 (m, 4H), 1.68 (m, 2H), 1.93 (m, 2H), 3.13 (s, 3H), 3.31 (s, 3H), 3.53 (s, 3H), 4.10 (m, 1H), 6.76 (d, 1H, $J = 7.2$ Hz); ^{13}C NMR (Bruker Avance III 600, $\text{DMSO}-d_6$) δ 23.4, 27.1, 29.2, 29.8, 32.4, 54.2, 101.7, 148.3, 150.9, 152.8, 153.8; ESI-HRMS m/z : calcd for $\text{C}_{13}\text{H}_{20}\text{N}_5\text{O}_2$ (MH^+), 278.1617, found 278.1612; Purity (HPLC): 96%.

4.4. Methylation of the C8-substituted aminocaffeine analogues (5a–b)

Potassium hydroxide (0.05 g) was powdered and suspended in 5 mL DMSO. The resulting mixture was stirred for 30 min at room temperature and the aminocaffeine analogue (3 mmol), dissolved in DMSO (5 mL), was added. The reaction was heated to 40 °C (in order for the aminocaffeine analogue to remain in solution) and iodomethane (0.8 mmol) was added. Stirring of the reaction was continued and another portion of iodomethane (0.8 mmol) was added every 20 min until silica gel TLC (petroleum ether/ethyl acetate 30:70) indicated completion of the reaction. The pH of the reaction was also continually measured, and when acidic (pH paper), another portion of potassium hydroxide (0.05 g) was added. Upon completion, the reaction was cooled to

room temperature and water (250 mL) was added. The resulting solution was incubated for several days at 4 °C and the formed crystals were collected by filtration.

4.4.1. 8-[Methyl(2-phenylethyl)amino]caffeine (5a)

The title compound was prepared from 8-[(2-phenylethyl)amino]caffeine (**4c**) and iodomethane in a yield of 57.7%: mp 103 °C (ethanol). ¹H NMR (Bruker Avance III 600, DMSO-*d*₆) δ 2.88 (t, 2H, *J* = 7.5 Hz), 2.98 (s, 3H), 3.16 (s, 3H), 3.33 (s, 3H), 3.47 (t, 2H, *J* = 7.5 Hz), 3.59 (s, 3H), 7.18 (m, 1H), 7.25 (m, 4H); ¹³C NMR (Bruker Avance III 600, DMSO-*d*₆) δ 27.3, 29.3, 32.5, 33.0, 38.6, 54.5, 103.8, 126.1, 128.3, 128.8, 139.0, 147.1, 150.9, 153.5, 156.6; ESI-HRMS *m/z*: calcd for C₁₇H₂₂N₅O₂ (MH⁺), 328.1774, found 328.1734; Purity (HPLC): 99%.

4.4.2. 8-[Methyl(4-phenylbutyl)amino]caffeine (5b)

The title compound was prepared from 8-[(4-phenylbutyl)amino]caffeine (**4e**) and iodomethane in a yield of 49.9%: mp 114 °C (ethanol). ¹H NMR (Bruker Avance III 600, DMSO-*d*₆) δ 1.57 (m, 4H), 2.57 (t, 2H, *J* = 7.15 Hz), 2.90 (s, 3H), 3.16 (s, 3H), 3.26 (t, 2H, *J* = 7.15 Hz), 3.32 (s, 3H), 3.65 (s, 3H), 7.15 (m, 3H), 7.24 (t, 2H, *J* = 7.91 Hz); ¹³C NMR (Bruker Avance III 600, DMSO-*d*₆) δ 26.3, 27.3, 27.9, 29.3, 32.6, 34.7, 38.4, 52.5, 103.8, 125.7, 128.2, 128.2, 142.0, 147.1, 150.9, 153.5, 156.9; ESI-HRMS *m/z*: calcd for C₁₉H₂₆N₅O₂ (MH⁺), 356.2087, found 356.2088; Purity (HPLC): 98%.

4.5. IC₅₀ determinations for the inhibition of human MAO

Microsomal preparations from insect cells containing recombinant human MAO-A and -B (5 mg/mL) served as enzyme sources and all enzymatic reactions were conducted in potassium phosphate buffer (100 mM, pH 7.4, made isotonic with KCl) to a final volume of 500 μL.¹⁹ The reactions contained the MAO-A/B mixed substrate, kynuramine, at concentrations of 45 μM and 30 μM for the incubations with MAO-A and -B, respectively, various concentrations of the test inhibitor (0–100 μM) and the MAO enzymes (0.0075 mg/mL). The enzyme activities employed for the IC₅₀ value determinations were 24–28 nmoles 4-hydroxyquinoline formed/min/mg protein for MAO-A and 6–8 nmoles 4-hydroxyquinoline formed/min/mg protein for MAO-B. Stock solutions of the test inhibitors were prepared in DMSO and added to the reactions to yield a final concentration of 4% (v/v) DMSO. The enzyme reactions were incubated at 37 °C for 20 min and then terminated with the addition of 400 μL NaOH (2 N) and 1000 μL distilled water. After centrifugation at 16,000g for 10 min, the fluorescence of the MAO generated 4-hydroxyquinoline in the supernatant fractions were measured ($\lambda_{\text{ex}} = 310 \text{ nm}$, $\lambda_{\text{em}} = 400 \text{ nm}$). To determine the concentrations of 4-hydroxyquinoline, a linear calibration curve was constructed from solutions of 4-hydroxyquinoline (0.047–1.50 μM) in potassium phosphate buffer. The calibration standards were prepared to a volume of 500 μL and contained 4% DMSO, 400 μL NaOH (2 N) and 1000 μL distilled water. The initial rate of MAO catalysis was plotted versus the logarithm of the inhibitor concentration to obtain a sigmoidal dose-response curve. Each curve was constructed from 6 different inhibitor concentrations spanning at least 3 orders of magnitude. These data were fitted to the one site competition model incorporated into the GraphPad Prism software and the IC₅₀ values were determined in triplicate and are expressed as mean ± standard deviation (SD).

4.6. Time-dependent inhibition studies

The reversibility of MAO inhibition was examined by determining the time-dependence of inhibition of three selected inhibitors, **3f**, **4g** and **5b**. The selected inhibitors were preincubated in potas-

sium phosphate buffer (100 mM, pH 7.4, made isotonic with KCl) with MAO-A and -B (0.015–0.03 mg/mL) for periods of 0, 15, 30, 60 min at 37 °C. The concentrations of the inhibitors used were 2-fold their measured IC₅₀ values for the inhibition of the respective MAO enzymes and were: 5.22 μM (**3f**) and 11.56 μM (**4g**) for the studies with MAO-A, and 0.32 μM (**3f**) and 5.94 μM (**5b**) for the studies with MAO-B. To compensate for a potential time-dependent loss of enzyme activity, the enzyme preincubations were firstly incubated at 37 °C and the inhibitors were subsequently added at different time points. These time points were selected as to ensure that all enzyme preparations were preheated at 37 °C for exactly 60 min, irrespective of the time period (0–60 min) for which the enzyme preparations were preincubated in the presence of the test inhibitor. These reactions were diluted 2-fold by the addition of kynuramine at concentrations of 45 and 30 μM for the incubations with MAO-A and -B, respectively, and the resulting reactions (500 μL final volume) were incubated at 37 °C for a further 15 min. The final enzyme concentration in these reactions was 0.0075–0.015 mg/mL and the concentrations of the selected inhibitors were approximately equal to their IC₅₀ values for the inhibition of the respective isozymes. The reactions were terminated with the addition of 400 μL NaOH (2 N) and 1000 μL distilled water and the rates of MAO catalyzed generation of 4-hydroxyquinoline were measured and calculated as described above. All measurements were carried out in triplicate and are expressed as mean ± SD.²³

4.7. Construction of Lineweaver–Burk plots

A set consisting of four Lineweaver–Burk plots were constructed for the inhibition of MAO-A and -B by the selected inhibitor **3f**. One plot was constructed in the absence of inhibitor while three plots were constructed in the presence of three different concentrations of **3f** each. These concentrations were 1.31–5.22 and 0.04–0.16 μM for the inhibition studies with MAO-A and -B, respectively. Four different kynuramine concentrations (15–90 μM) were employed for each plot and the concentrations of recombinant human MAO-A and -B used were 0.015 mg/mL. The initial MAO catalytic rates were measured as described above. Linear regression analysis was performed using GraphPad Prism.²³

4.8. Molecular modeling studies

The modeling studies were carried out with the Windows based Discovery Studio 1.7 molecular modeling software (Accelrys).^{23,27} For this purpose the crystallographic structures of MAO-A co-crystallized with harmine (PDB code: 2Z5X)³ and MAO-B co-crystallized with safinamide (PDB code: 2V5Z)⁴ were obtained from the Brookhaven Protein Data Bank (www.rcsb.org/pdb). The protonation states of the ionizable amino acids residues were calculated at pH 7.4 and hydrogen atoms were added to the receptor models. The valences of the FAD cofactors (oxidized state) and co-crystallized ligands were corrected and hydrogen atoms were added according to the appropriate protonation states at pH 7.4. The structures were typed automatically with the Momany and Rone CHARMm forcefield, the backbone of the protein was constrained and the structures were subjected to a three step energy minimization. The first step was a steepest descent minimization which was followed by conjugate gradient minimization. For both protocols the termination criteria was set to a maximum of 2500 steps or a minimum value of 0.1 for the root mean square of the energy gradient. The final step was an adopted basis Newton–Rapheson minimization and the termination criteria was set to a maximum of 5000 steps or a minimum value for the root mean square of the energy gradient of 0.01. For these minimization steps the implicit generalized Born solvation model with simple switching was em-

ployed with the dielectric constant set to 4. For both the MAO-A and -B models, the crystal water molecules were removed with the exception of three active site waters in each model. The X-ray crystallographic structures of MAO-B shows that three active site water molecules (HOH 1155, 1170 and 1351; A-chain) are conserved, all located in the vicinity of the FAD cofactor.⁴ In the MAO-A model, the crystal waters HOH 710, 718 and 739 which occupies the analogous positions in the MAO-A active site compared to those cited above for MAO-B, were retained. The co-crystallized ligands and the backbone constraints were subsequently removed from the models and the binding sites were identified by a flood-filling algorithm. The structures of **3a–c** and **4c** were constructed within Discovery Studio, and their hydrogen atoms were added according to the appropriate protonation states at pH 7.4. The geometries of the ligands were briefly optimized in Discovery Studio using a fast Dreiding-like forcefield (1000 iterations) and the atom potential types and partial charges were assigned with the Momany and Rone CHARMM forcefield. Docking of the ligands was carried out with the LigandFit application of Discovery Studio and the docking solutions were refined using the Smart Minimizer algorithm. The parameters for the docking runs were set to their default values, ten possible binding solutions were computed for each docked ligand and the best-ranked binding conformation of each ligand was determined according to the DockScore values. The illustrations were prepared in PyMOL.²⁸ It is interesting to note that among the 10 best ranked binding orientations, there were orientations which exhibited a reversed binding mode with the caffeine ring directed towards the entrance of the MAO-A and -B active sites while the C8 sulfanyl and amino side chains project towards the FAD cofactor. Based on the low DockScore values these orientations were however deemed unlikely.

Acknowledgments

The NMR spectra were recorded by André Joubert of the SASOL Centre for Chemistry, North-West University while the MS spectra were recorded by the Mass Spectrometry Service, University of the Witwatersrand and the Mass Spectrometry Unit, Stellenbosch University. This work was supported by grants from the National Research Foundation and the Medical Research Council, South Africa.

Supplementary data

Supplementary data associated with this article can be found, in the online version, at doi:10.1016/j.bmc.2011.10.036.

References and notes

1. Binda, C.; Newton-Vinson, P.; Hubálek, F.; Edmondson, D. E.; Mattevi, A. *Nat. Struct. Biol.* **2002**, *9*, 22.
2. Shih, J. C.; Chen, K.; Ridd, M. J. *Annu. Rev. Neurosci.* **1999**, *22*, 197.
3. Son, S.-Y.; Ma, J.; Kondou, Y.; Yoshimura, M.; Yamashita, E.; Tsukihara, T. *Proc. Natl. Acad. Sci. U.S.A.* **2008**, *105*, 5739.
4. Binda, C.; Wang, J.; Pisani, L.; Caccia, C.; Carotti, A.; Salvati, P.; Edmondson, D. E.; Mattevi, A. *J. Med. Chem.* **2007**, *50*, 5848.
5. Youdim, M. B. H.; Edmondson, D.; Tipton, K. F. *Nat. Rev. Neurosci.* **2006**, *7*, 295.
6. Nicotra, A.; Pierucci, F.; Parvez, H.; Senatori, O. *Neurotoxicology* **2004**, *25*, 155.
7. Fowler, J. S.; Volkow, N. D.; Wang, G. J.; Logan, J.; Pappas, N.; Shea, C.; MacGregor, R. *Neurobiol. Aging* **1997**, *18*, 431.
8. Youdim, M. B. H.; Collins, G. G. S.; Sandler, M.; Bevan-Jones, A. B.; Pare, C. M.; Nicholson, W. J. *Nature* **1972**, *236*, 225.
9. Collins, G. G. S.; Sandler, M.; Williams, E. D.; Youdim, M. B. H. *Nature* **1970**, *225*, 817.
10. Di Monte, D. A.; DeLanney, L. E.; Irwin, I.; Royland, J. E.; Chan, P.; Jakowec, M. W.; Langston, J. W. *Brain. Res.* **1996**, *738*, 53.
11. Finberg, J. P.; Wang, J.; Bankiewicz, K.; Harvey-White, J.; Kopin, I. J.; Goldstein, D. S. *J. Neural Transm. Suppl.* **1998**, *52*, 279.
12. Fernandez, H. H.; Chen, J. J. *Pharmacotherapy* **2007**, *27*, 174S.
13. Youdim, M. B. H.; Bakhle, Y. S. *Br. J. Pharmacol.* **2006**, *147*, S287.
14. Van der Walt, E. M.; Milczek, E. M.; Malan, S. F.; Edmondson, D. E.; Castagnoli, N., Jr.; Bergh, J. J.; Petzer, J. P. *Bioorg. Med. Chem. Lett.* **2009**, *19*, 2509.
15. Strydom, B.; Malan, S. F.; Castagnoli, N.; Bergh, J. J.; Petzer, J. P. *Bioorg. Med. Chem.* **2010**, *18*, 1018.
16. Strydom, B.; Bergh, J. J.; Petzer, J. P. *Eur. J. Med. Chem.* **2011**, *46*, 3474.
17. Long, L. M. *J. Am. Chem. Soc.* **1947**, *69*, 2939.
18. Cramer, L. *Chem. Ber.* **1894**, *27*, 3089.
19. Novaroli, L.; Reist, M.; Favre, E.; Carotti, A.; Catto, M.; Carrupt, P. A. *Bioorg. Med. Chem.* **2005**, *13*, 6212.
20. Prins, L. H. A.; Petzer, J. P.; Malan, S. F. *Eur. J. Med. Chem.* **2010**, *45*, 4458.
21. Tipton, K. F.; Boyce, S.; O'Sullivan, J.; Davey, G. P.; Healy, J. *Curr. Med. Chem.* **2004**, *11*, 1965.
22. Fowler, J. S.; Volkow, N. D.; Logan, J.; Wang, G.; MacGregor, R. R.; Schlyer, D.; Wolf, A. P.; Pappas, N.; Alexoff, D.; Shea, C.; Dorflinger, E.; Kruchow, L.; Yoo, K.; Fazzini, E.; Patlak, C. *Synapse* **1994**, *18*, 86.
23. Manley-King, C. I.; Bergh, J. J.; Petzer, J. P. *Bioorg. Med. Chem.* **2011**, *19*, 261.
24. Binda, C.; Mattevi, A.; Edmondson, D. E. *J. Biol. Chem.* **2002**, *277*, 23973.
25. Hubálek, F.; Binda, C.; Khalil, A.; Li, M.; Mattevi, A.; Castagnoli, N., Jr.; Edmondson, D. E. *J. Biol. Chem.* **2005**, *280*, 15761.
26. Vlok, N.; Malan, S. F.; Castagnoli, N., Jr.; Bergh, J. J.; Petzer, J. P. *Bioorg. Med. Chem.* **2006**, *14*, 3512.
27. Accelrys Discovery Studio 1.7, Accelrys Software Inc., San Diego, CA, USA, 2006. <http://www.accelrys.com>.
28. DeLano, W. L. The PyMOL Molecular Graphics System. DeLano Scientific, San Carlos, USA, 2002.